

# Laser setup for measuring ground-level turbulence

**L Yatcheva, R Barros, S Keary and S Gladysz**

Fraunhofer Institute of Optronics, System Technologies and Image Exploitation IOSB  
Gutleuthausstraße 1, 76275 Ettlingen, Germany

E-mail: lydia.yatcheva@iosb.fraunhofer.de

**Abstract.** Ground-level turbulence is usually strong and can thus be a limiting factor for many applications such as laser communications or astronomical observations. In this paper, the working principle of a setup for characterization of optical turbulence along a horizontal path in the lower boundary layer is described. The system includes a telescope focusing a laser beam onto a retro-reflector located at a distance of 410 meters as well as an optical test-bench comprising two cameras and a Shack-Hartmann wavefront sensor. Some of the challenges encountered when using this type of sensor for measurement of strong turbulence are discussed. Furthermore, two techniques for estimation of Fried's coherence length  $r_0$  are presented and their results compared.

## 1. Introduction

Electro-optical systems, whether used for astronomical observations [1], remote-sensing and surveillance from space [2], tracking and high-resolution imaging of satellites [3], delivery of directed energy to space-based platforms [4], or horizontal-path imaging and laser communications [5], are always affected by atmospheric turbulence and in the majority of cases this turbulence imposes a fundamental limitation to their performance. Measurements of optical turbulence have a long tradition, from qualitative observations made by Newton [6] up to large scale measurement campaigns in preparation for the construction of future 30-m class optical telescopes [7].

It is well known that turbulence near the ground is usually the strongest. Still, the influence of turbulence on adaptive optics (AO) systems in this layer is rarely investigated. Our focus is laser propagation near the ground and for this application an experimental setup for turbulence measurement, characterization and testing of advanced wavefront sensing modalities was built [8]. The system includes a telescope to focus a laser beam onto a retro-reflector located at a distance of 410 meters, and an optical test-bench to measure wavefronts and focal-plane images, as well as pupil-plane intensity fluctuations of the reflected beam. The setup allows the collection of motion-corrected point-spread functions, individual wavefronts from the Shack-Hartmann sensor, and scintillation data, all simultaneously. In this paper the design of the experiment and the methods for determination of turbulence strength are discussed and some shortcomings of the Shack-Hartmann wavefront sensor under strong turbulence conditions are shown. In the future the setup will be used as the main optical system for testing of the holographic wavefront sensor [9].

## 2. Design of the setup

The concept of the system and its current implementation are shown in figure 1. The setup was designed and optimized to work in the visible spectrum ( $\lambda = 632.8$  nm). However, for the purpose of



free-space laser communications, further modifications will be made in order to operate in the near-infrared wave band ( $\lambda = 1.55 \mu\text{m}$ ). In the present configuration, a Gaussian beam leaving the 30-cm aperture is focused on the retro-reflector while propagating through a random medium (air), and is reflected back to the transmitter through the same instance of the random medium (figure 1a).

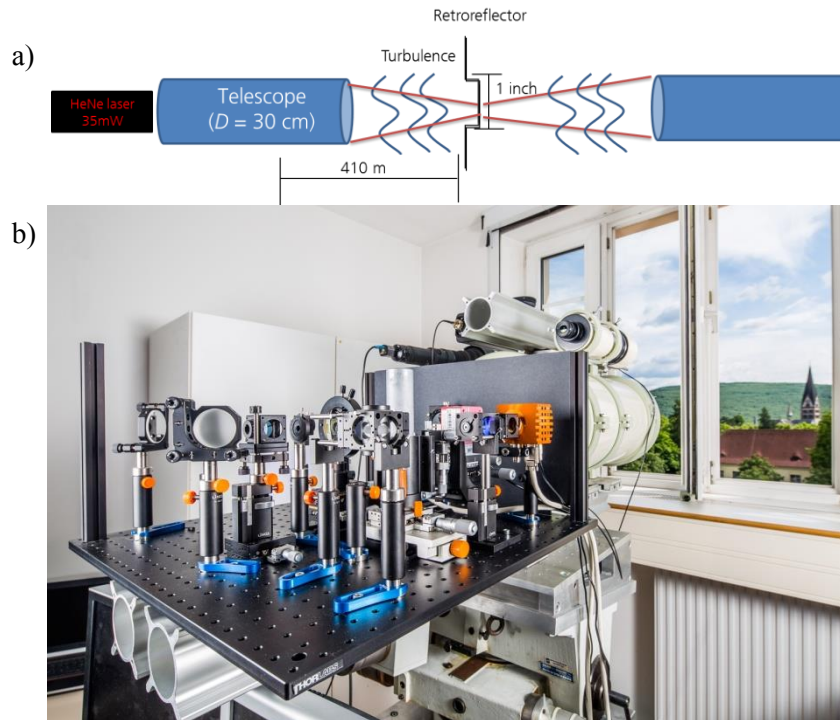


**Figure 1.** a) System concept: propagation geometry of the beam. b) Photograph of the experimental setup: test-bench, telescope and in the background the church tower where the reflector is located.

The corner cube retro-reflector rotates the wavefront by 180 degrees and sends it back in the direction of the transmitter. Thus, the setup is in principle a monostatic one albeit the area of the pupil where the coherence and subsequently intensity would be amplified by the double-pass propagation [10] is blocked by a large central obscuration of our Dall-Kirkham telescope. Since the peripheral parts of the wavefront are flipped horizontally and vertically upon reflection from the corner cube, it is assumed that statistics derived from these annular wavefronts will correspond to 820 m propagation of (almost) completely uncorrelated turbulence. Naturally, one must remember that in this particular case light is focused in the middle of the path and therefore the presented values of Fried's parameter correspond to such a propagation geometry only. Additionally, the retro-reflector sends light in the exact direction it originated from which makes the system insensitive to atmospheric tip and tilt.

Figure 2 depicts the optical setup schematically. The system is fed by a 35 mW linearly polarized, red laser beam that is focused by a converging lens (lens 1) on the image plane of the Dall-Kirkham telescope (Mewlon 300). The latter is conjugated with the retro-reflector plane located at the church tower 410 m away. Before leaving the system, the beam passes through a half-waveplate and is reflected by a polarizing beamsplitter (BS) through a quarter-waveplate. Thus the now circularly polarized beam travels to the reflector and back, and upon the second passage through the quarter-waveplate, has the opposite polarization with respect to the initial one. The incoming light can thus be collected by the telescope and re-collimated by a second lens (lens 2). A pellicle beam-splitter (BS 2) after the second lens produces two images of the entrance pupil of the telescope. One is dedicated to the Shack-Hartmann wavefront sensor (SHWFS) while the other is imaged again by a relay system (lenses 3 and 4) onto a high-speed camera for the purpose of scintillation measurements. Another

beamsplitter (BS3) and a further detector placed at the focal plane of lens 3 allow concurrently measuring the focal plane image corresponding to a point spread function (PSF).

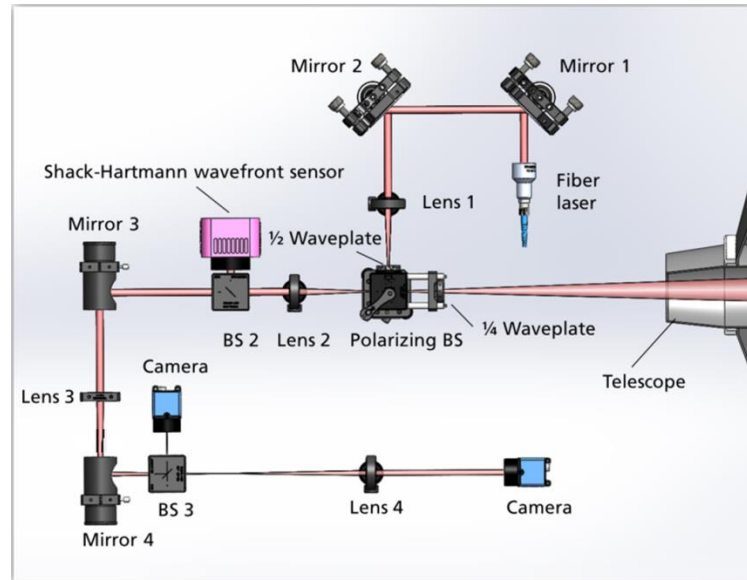


**Figure 2.** Detailed scheme of the optical test-bench.

The wavefront sensor used is SHSCAM from Optocraft with a 1.4-Megapixel, 8-bit greyscale Photonfocus sensor, with a frame rate set to 38 Hz and a square pattern lenslet array consisting of 42×31 lenslets with a pitch of 248 μm. PSF images are collected using a DCC3240M camera from Thorlabs, running at 100 fps. The exposure time for all cameras was set to 2 ms.

The measurements delivered by SHWFS and the PSF-camera are the subject of this paper. The scintillation index analysis is not described here as it has been presented in [8].

### 3. Turbulence strength estimation

For the purpose of this work, Fried's coherence length ( $r_0$ ) was chosen to quantify turbulence strength under the propagation geometry shown in figure 1a. Two approaches for measurement estimation of  $r_0$  are analyzed: Zernike mode variances fitting and fitting of the modulation transfer function (MTF). In the following, the methods are described in more detail.

#### 3.1. Zernike variances

One approach for measuring turbulence strength involves estimation of  $r_0$  based on the variance of Zernike modes [11].

For Kolmogorov turbulence, regardless of propagation geometry, it can be shown that the variance of any Zernike mode  $Z_n$  in radial order  $n$  can be represented as [12]:

$$Z_n = 1.095 (n + 1) \frac{\Gamma[-5/6 + n] \Gamma[7/3]}{\Gamma[23/6 + n] \Gamma[17/6]} \left(\frac{D}{r_0}\right)^{5/3} \quad (1)$$

where  $\Gamma$  is the gamma function and  $D$  is the telescope diameter.

Throughout the course of an experiment, the first 25 Zernike modes are recorded in regular intervals. Variances are computed for sets of 1000 measurements and compared to the corresponding theoretical values for different  $r_0$  in accordance with the model. Thus, Fried's coherence length is obtained by the best fit to experimental data.

### 3.2. Fried's "short-exposure" MTF

The second method of estimating turbulence strength is based on Fourier optics.

Fried [13] derived a theoretical model for the tip-tilt-corrected ("short-exposure") MTF. In this theory, ensemble-averaged MTF, i.e., the Fourier transform of the PSF, is given by:

$$\mathbf{H}_s(\vec{u}) = \mathbf{H}_0(\vec{u}) \times \mathbf{H}_{SE}(\vec{u}) \quad (2)$$

where  $\mathbf{H}_{SE}(\vec{u})$  is the average short-exposure MTF of the atmosphere only, and  $\mathbf{H}_0(\vec{u})$  is the telescope's MTF ( $\vec{u}$  is the two-dimensional spatial frequency). For a diffraction-limited circular aperture of diameter  $D$  we have:

$$\mathbf{H}_0(\vec{u}) = \frac{2}{\pi} \left[ \arccos\left(\frac{\bar{\lambda}zu}{D}\right) - \frac{\bar{\lambda}zu}{D} \sqrt{1 - \left(\frac{\bar{\lambda}zu}{D}\right)^2} \right] \quad (3)$$

where  $u = |\vec{u}|$ ,  $\bar{\lambda}$  is the average wavelength, and  $z$  is the distance from the exit pupil to the image plane. For the presented work, this approximation, although neglecting the central obscuration of the pupil and Gaussian apodization, was found to yield satisfactory results.

Furthermore, Fried postulated that:

$$\mathbf{H}_{SE}(\vec{u}) = \exp \left\{ -3.44 \left( \frac{\bar{\lambda}zu}{r_0} \right)^{5/3} \left[ 1 - \alpha \left( \frac{\bar{\lambda}zu}{D} \right)^{1/3} \right] \right\} \quad (4)$$

where  $\alpha$  is a parameter that varies between 1/2 when there are both intensity and phase variations across the collecting aperture and 1 when only phase distortions are present.

The method consists therefore of building up a temporal-average PSF, Fourier transforming it, and comparing it to a set of templates, based on equations (2) – (4). Since varying  $\alpha$  was found not to affect the measurement result significantly, the only free parameter in these models is  $r_0$  and thus the template that best fits the data automatically yields turbulence strength.

## 4. Efficacy of the Shack-Hartmann wavefront sensing in strong turbulence

The Shack-Hartmann wavefront sensor is a reliable and widely used solution in astronomical adaptive optics (AO). However, two fundamental characteristics can inhibit the application of this sensor to more challenging scenarios like laser propagation over long horizontal paths within extended-volume turbulence that causes scintillation and branch points in the wavefronts [14].

Firstly, due to the procedure of wavefront reconstruction the bandwidth of SHWFS is limited. This has consequences for deploying SHWFS-based AO systems on moving platforms and/or for satellite tracking. Secondly, SHWFS is highly sensitive to scintillation effects. Obscurements or saturations of parts of the sensor's pupil can lead to failure rate of the wavefront reconstruction process. We demonstrate the onset of this effect in figure 3 where circles denote either the errors signalled by the SHWFS software (gaps in the time series) or the ones which are easy to spot by eye but have not been flagged as errors by the software (sharp peaks and dips in the data).

Given this reservation, one needs to use datasets which were not corrupted by errors or such where errors could be quickly identified and removed.

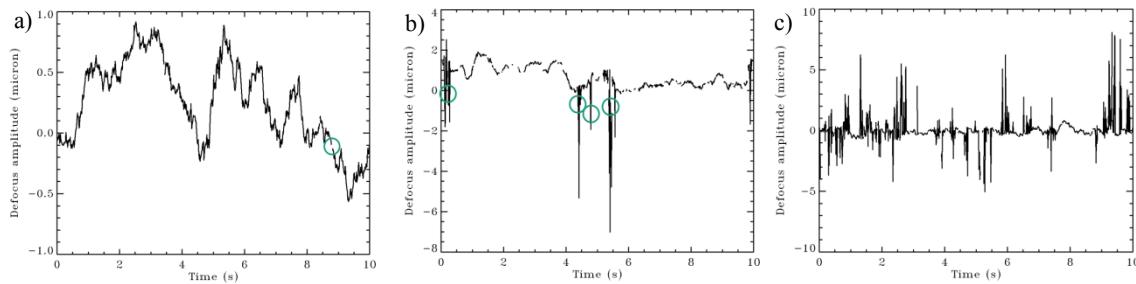


**Figure 3.** Values of defocus given by the Shack-Hartmann wavefront sensor at 9 am (a), 10 am (b) and 11 am (c) on the 21<sup>st</sup> of October 2014. In each panel 10 s of measurements are plotted. Please note the different scales. Turbulence is generally increasing from early morning until midday and then decreasing again. Consequently, errors can increase throughout the day as well. The presented data from 11 o'clock contains predominantly erroneous measurements and is thus difficult to draw conclusions from.

### 5. Experimental results

The two methods were numerically implemented and tested experimentally. Figure 4 shows a comparison of the yielded values throughout the course of one morning. A fairly good agreement between the values can be observed.

One should note, however, that turbulence did not vary significantly during this experiment, with an average  $r_0$  of 7.1 mm and 7.8 mm for the MTF and Zernike fitting methods respectively. This was mainly due to the nearly constant meteorological conditions during the measurement time, with the temperature changing less than 2 °C.

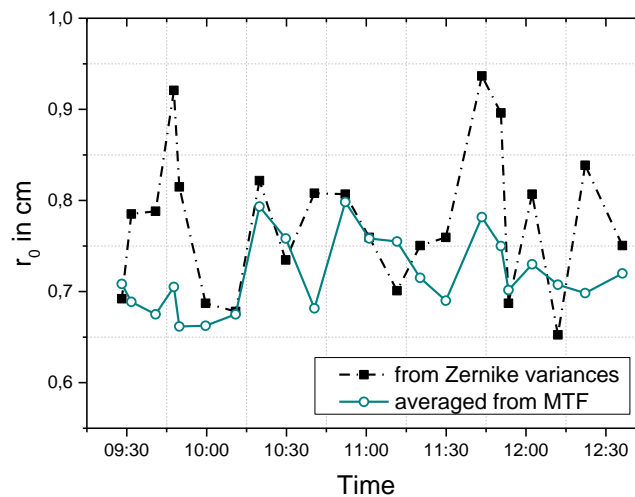


**Figure 4.** Comparison of the two estimation methods. Measurements from the 8<sup>th</sup> of December 2014. Dash-dotted line and square data points represent the values obtained from the Zernike variance fitting for sets of 1000 frames, while solid line and hollow circular data points depict values from averaging three subsequent sets of 3000 frames.

### 6. Conclusions and outlook

A laser setup capable of measuring turbulence on a horizontal urban path was successfully implemented and results from fitting of Zernike mode variances and modulation transfer functions were found to be in agreement despite some challenges of using the Shack-Hartmann sensor for this application. In the future, a portable measurement system, based on the same principles, would allow characterizing turbulence at different sites, e.g. in a telescope dome [15].

Furthermore, the assumption of Kolmogorov turbulence near the ground shall be investigated using the Shack-Hartmann angle-of-arrival structure functions [16]. Additionally, novel wavefront sensing modalities could be implemented [17]. Finally, the shortcomings of the Shack-Hartmann wavefront sensor could be compensated using a different device, such as e.g. the holographic wavefront sensor which is insensitive to scintillation [9].

## References

- [1] Davies R and Kasper M 2012 Adaptive optics for astronomy *Annual Review of Astronomy and Astrophysics* **50** 1-47
- [2] Hajlaoui N, Chauv C, Perrin G, Falzon F and Benazza-Benyahia A 2010 Satellite image restoration in the context of a spatially varying point spread function *J. Opt. Soc. Am. A* **27** 1473-81
- [3] Matson C L, Borelli K, Jefferies S, Beckner J C C, Hege E K and Lloyd-Hart M 2009 Fast and optimal multiframe blind deconvolution algorithm for high-resolution ground-based imaging of space objects *Appl. Opt.* **48** A75-A92
- [4] Murphy D V 1992 Atmospheric-turbulence compensation experiments using cooperative beacons *Lincoln Laboratory Journal* **5** 25-44
- [5] Vorontsov M, Riker J, Carhart G, Gudimetla V S R, Beresnev L, Weyrauch T and Roberts L C Jr 2009 Deep turbulence effects compensation experiments with a cascaded adaptive optics system using a 3.63 m telescope *Appl. Opt.* **48** A47-A57
- [6] Newton I, 1952 Optics *Great Books of the Western World* vol 34 ed R M Hutchins (Chicago: Encyclopedia of Britannica)
- [7] Schoeck M *et al.* 2009 Thirty meter telescope site testing I: overview *Publications of the Astronomical Society of the Pacific* **121** no 878 384-395
- [8] Barros R, Keary S, Yatcheva L, Toselli I and Gladysz S 2014 Experimental setup for investigation of laser beam propagation along horizontal urban path *Proc. of SPIE* **9242** 92421L
- [9] Palomo P M, Zepp A and Gladysz S 2014 Characterization of the digital holographic wavefront sensor *Proc. of SPIE* **9242** 92421T
- [10] Nelson W, Palastro J P, Wu C and Davis C C 2014 Enhanced backscatter of optical beams reflected in atmospheric turbulence *Proc. of SPIE* **9224** 922411
- [11] Noll R J 1976 Zernike polynomials and atmospheric turbulence *J. Opt. Soc. Am.* **66** no 3 207-11
- [12] Sasiela R J 2007 *Electromagnetic wave propagation in turbulence: evaluation and application of Mellin Transforms* 2nd ed (Bellingham, Washington USA: SPIE Press)
- [13] Fried D L 1966 Optical resolution through a randomly inhomogeneous medium for very long and very short exposures *J. Opt. Soc. Am.* **56** 1372-79
- [14] Zepp A, Gladysz S and Stein K 2013 Holographic wavefront sensor for fast defocus measurement *J. Adv. Opt. Technol.* **2** 433-37
- [15] Berdja A, Guzman D, Saez N, David N, Dubost N, Sarazin M and Ziad A 2014 LOTUCE2: a dome-seeing instrument for the E-ELT *Proc. of SPIE* **9147** 91479R-1
- [16] Nicholls T W, Boremann G D and Dainty J 1995 Use of a Shack-Hartmann wave-front sensor to measure deviations from a Kolmogorov phase spectrum *Optics letters* **20** no 24 2460-62
- [17] Polans J, McNabb R P, Izatt J A and Farsiu S 2014 Compressed wavefront sensing *Optics letters* **39** no 5 1189-92